Residual frequency drift in an atomic fountain clock

Yuanbo Du (杜远博)[1,2], Rong Wei (魏 荣)[1,*], Richang Dong (董日昌)[1,2], Fan Zou (邹 凡)[1,2], Jinda Lin (林锦达)[1], Wenli Wang (王文丽)[1], and Yuzhu Wang (王育竹)[1]

[1]*Key Laboratory of Quantum Optics, Center for Cold Atom Physics, Shanghai Institute of Optics and Fine Mechanics, Chinese Academy of Science, Shanghai 201800, China*

[2]*University of Chinese Academy of Sciences, Beijing 100049, China*

**Corresponding author: weirong@siom.ac.cn*

Received April 12, 2015; accepted June 19, 2015; posted online July 27, 2015

We report a locking mode in which the local oscillator (LO) is locked to an atomic fountain and calibration of the residual frequency drift (RFD). In this running mode, the locked LO outputs a standard frequency signal, and a short-term fractional frequency stability of $2.7 \times 10^{-13}\tau^{-1/2}$ is achieved. Due to the frequency drift of the LO in free running mode, a systematic frequency bias, or RFD, exists after being locked by the atomic fountain. We analyze and measure the RFD with a value of $-3(2) \times 10^{-16}$. A sectionalized post-process method is adopted to calibrate the RFD.

OCIS codes: 120.0120, 270.0270, 120.3940.
doi: 10.3788/COL201513.091201.

Atomic fountains present excellent performance and have become the most accurate primary frequency standards running in the international atomic time (TAI) system and in main time-keeping organizations over the world[1–6]. Most of the fountains do not run independently, but function as part of a clock group, and utilize other oscillators steered by active H-masers as their local oscillators (LOs)[6–8]. They record the frequency error of the LO with respect to an atomic fountain rather than outputting a standard frequency signal. This mode is suitable for atomic fountains in the time-keeping fields. However, in many fields of high-precision measurements, atomic fountains operated in the LO locking mode (LOL) are also required. In the LOL, the LO, usually a low phase-noise crystal oscillator, is directly locked by the atomic fountain, and outputs a standard frequency signal. For instance, in the Physikalisch-Technische Bundesanstalt (PTB) metrology institute, a voltage-controlled quartz oscillator was locked to the atomic CsF1 fountain and provided a standard frequency signal with a fractional frequency stability of $3.5 \times 10^{-13}\tau^{-1/2}$[9]. In addition, FOM, the transportable fountain of the Laboratoire national de métrologie et d'essais—Système de Références Temps-Espace (LNE-SYRTE) running in LOL, has been moved to different laboratories to fulfill many physics experiments that extend the application of atomic fountains[10,11].

In this work, an oven controlled crystal oscillator (OCXO) serves as the LO of our atomic fountain clock (AFC), and is locked on the resonance spectrum of the atomic fountain. The locked LO provides a standard frequency signal whose performance is measured by comparing with a local active H-maser. The short-term fractional frequency stability of $2.7 \times 10^{-13}\tau^{-1/2}$ obtained is close to that of main primary frequency standards[7,8,12]. In the LOL, the time-dependent intrinsic frequency drift of the LO induces an additional systematic bias and uncertainty of the AFC. We measure the systematic bias with an order of 10^{-16}. In addition, we adopt a sectionalized post-process method to calibrate the systematic bias, and experimental results show that the effect due to variation of the systematic bias is suppressed after the calibration. The standard frequency signal of our AFC provides a frequency reference that makes it possible to launch other high-precision measurements.

The schematic diagram of our rubidium AFC is illustrated in Fig. 1(a). An OCXO (BVA-8607, OSA. Corp.) acts as a LO, the frequency output of which is transferred to the microwave synthesizer to provide the microwave to interrogate the cold atoms in the AFC. Two ADCs are used to collect the time of flight (TOF) signals of cold atoms in the $F = 1$ and $F = 2$ hyperfine levels of ^{87}Rb after the microwave interrogation process. According to the frequency error signal y_e computed from the TOF signals and the appropriate feedback parameters from the proportional integral (PI) electronics, a control voltage is derived and sent to a homemade low-noise electronic circuit based on a high-resolution (20-bit) digital to analog converter (DAC). Thus, the LO is locked on the resonance spectrum (Ramsey fringe) of the atomic fountain and it gives a standard frequency signal output. Meanwhile, the output of the LO is compared with an active H-maser (VCH-1003A) to measure the frequency difference between them.

In the AFC, the fountain cycle T_L is 1.853 s, and the Ramsey interrogation time T_I is 0.5 s, while the locking period is double the fountain cycle, about $2T_L = 3.706$ s, for the AFC is locked by square-wave modulation of the synthesizer output frequency in two successive fountain cycles[1]. After the LO is locked by the AFC, the short-term fractional frequency stability of the LO compared with the H-maser is $2.7 \times 10^{-13}\tau^{-1/2}$, which reaches 2.7×10^{-15} at the average time of 10000 s, as shown in Fig. 1(b). This experimental result is near the calculation limit of the fractional frequency stability determined by the phase

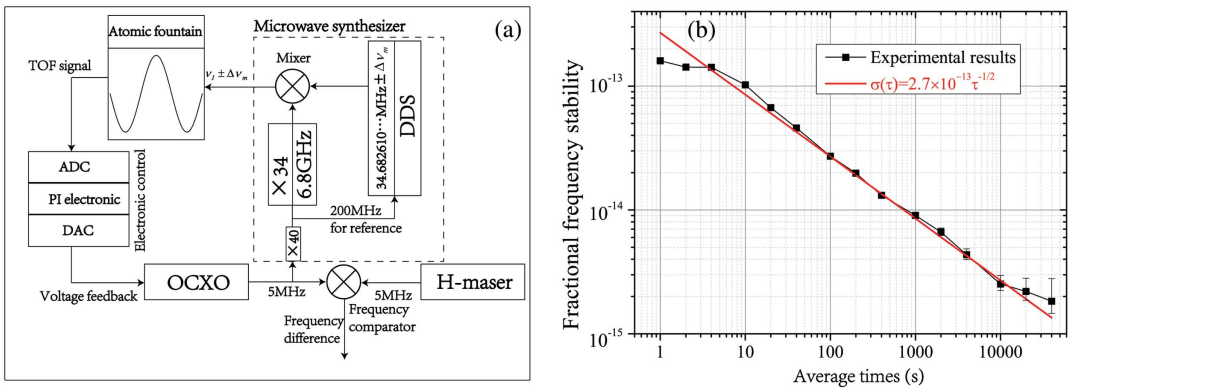

Fig. 1. (a) Simple schematic diagram of our AFC. The frequency output of the OCXO is transferred to the microwave synthesizer and the synthesizer provides the interrogation frequency for the atomic fountain, yielding a frequency error signal with the electronic control system locking the OCXO to the resonance spectrum of the fountain; simultaneously, the OCXO frequency output is compared with a local H-maser. ADC: analog to digital converter. (b) The short-term frequency stability of the locked LO with respect to the H-maser, with the fitting curve of $2.7 \times 10^{-13}\tau^{-1/2}$. It reaches 2.7×10^{-15} at the average time of 10000 s, and arrives at 1.8×10^{-15} at the average time of 40000 s.

noise of the LO[13] and the microwave synthesizer[14,15], which is $2.0 \times 10^{-13}\tau^{-1/2}$. In addition, the short-term stability index in our AFC is close to that of main AFCs in the world, such as $2.0 \times 10^{-13}\tau^{-1/2}$ of ITCsF2[7], $1.7 \times 10^{-13}\tau^{-1/2}$ of NPL-CsF2[8], and $1.7 \times 10^{-13}\tau^{-1/2}$ of NIST-F2[12]. Limited by the specification of H-masers, the comparison data tends to degenerate at longer average time scale, and it no longer represents the stability of the AFC.

In the process of LOL, the voltage controlling the LO has an observable drift, which is ascribed to the inherent attribute of OCXO aging[16]. The voltage drift rate is strictly determined by the frequency drift rate of the LO in free running mode. Based on the experimental data of voltage drift and the ratio of fractional frequency to control voltage of the LO (2.30×10^{-8}/V) during MJD 57080-57103, the equivalent fractional frequency drift of the LO in free running mode is obtained, as illustrated in Fig. 2(a), with a linear fitting of -1.01×10^{-16}/s. Within the typical locking period of our fountain, the fractional frequency drift of the LO is -3.74×10^{-16}. The characteristic frequency of drift during one locking period is beyond the locking bandwidth of the LOL, and thus cannot be compensated in the LOL, leading to a systematic bias. We name the uncompensated systematic bias caused by the frequency drift of LO during the locking period as residual frequency drift (RFD). In the scale of 10^{-16}, the RFD is large enough and becomes necessary to be taken into account in the evaluation of systematic biases of the AFC.

Without loss of generality, we assume the equivalent fractional frequency drift of the LO is in the linear relationship with time, say $y(t) = y_0 + \mathrm{D}t$, where y_0 is the average of the fractional frequency output of the LO at the starting of the first Ramsey interaction, and D is the fractional frequency drift rate. In the LOL, the tendency of frequency drift of the LO is suppressed, and the output of the LO is locked. The time evaluation of atoms populated

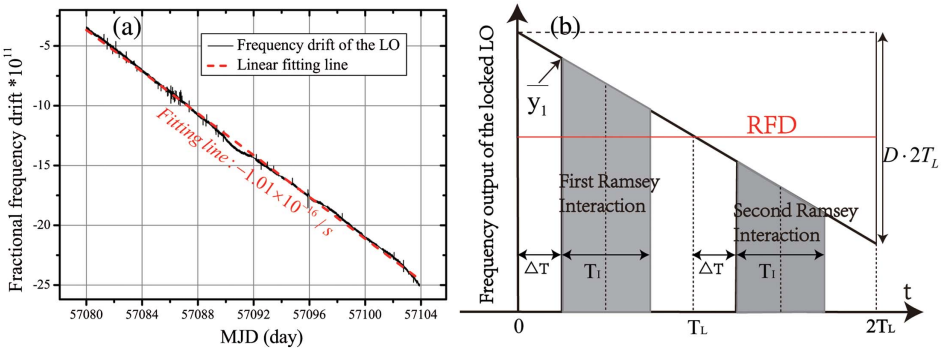

Fig. 2. (a) Equivalent fractional frequency drift of LO in free running during MJD 57080-57103, linear drift rate in fitting: -1.01×10^{-16}/s; (b) RFD scheme diagram of LO in a linear drift. $\overline{y_1}$ is the average of the fractional frequency output of LO at the start of the first Ramsey interaction, T_L is the fountain cycle of cold atoms, ΔT is the time before the Ramsey interaction in one fountain cycle, T_I is the Ramsey interaction time, while the areas with deep color represent two Ramsey interactions during two successive fountain cycles.

between two energy levels in the Ramsey interaction could be represented by the interaction picture as

$$\begin{pmatrix} c_1(T+2\tau) \\ c_2(T+2\tau) \end{pmatrix} = U(\Omega',\tau)\,U_{\text{free}}(\Delta,T)\,U(\Omega',\tau)\begin{pmatrix} c_1(0) \\ c_2(0) \end{pmatrix}, \tag{1}$$

$$U(\Omega',\tau) = \begin{pmatrix} \cos(\Omega'\tau/2) + i\Delta/\Omega'\,\sin(\Omega'\tau/2) & -i\Delta/\Omega'\,\sin(\Omega'\tau/2) \\ -i\Delta/\Omega'\,\sin(\Omega'\tau/2) & \cos(\Omega'\tau/2) - i\Delta/\Omega'\,\sin(\Omega'\tau/2) \end{pmatrix},$$

$$U_{\text{free}}(\Delta,T) = \begin{pmatrix} e^{i\Delta T/2} & 0 \\ 0 & e^{-i\Delta T/2} \end{pmatrix}.$$

where Ω' is the effective Rabi frequency, τ is atom-microwave interaction duration, and Δ is angular frequency detuning of microwave. Since there is still frequency drift during every locking period, as illustrated in Fig. 2(b), the equivalent free-evaluation matrix becomes

$$U_{\text{free}} = \begin{pmatrix} e^{i(2\pi\overline{y_1}+\pi DT_I)T_I} & 0 \\ 0 & e^{-i(2\pi\overline{y_1}+\pi DT_I)T_I} \end{pmatrix}, \tag{2}$$

where $\overline{y_1}$ is average in fractional frequency of the locked LO at the starte of the fountain cycle. Thus, the transition probabilities detected in two successive fountain cycles are, successively,

$$\begin{aligned} P_1 &\approx \frac{1}{2}[1 + (2\pi\overline{y_1} + \pi DT_I)\,T_I], \\ P_2 &\approx \frac{1}{2}[1 - (2\pi\overline{y_1} + 2\pi DT_L + \pi DT_I)\,T_I]. \end{aligned} \tag{3}$$

Correspondingly, average fractional frequency error detected in two successive fountain cycles is represented as

$$\overline{y_e} = \overline{y_1} + D(T_L + T_I)/2. \tag{4}$$

The frequency feedback is related to the detected frequency error y_e, and the average fractional feedback is $-(P+I)[\overline{y_1} + D(T_L+T_I)/2]$, where P and I are abbreviations for proportional and integral feedback coefficients, respectively. In LOL, the average of the fractional feedback equals the frequency drift during the locking period, say

$$(P+I)[\overline{y_1} + D(T_L+T_I)/2] = 2DT_L. \tag{5}$$

Correspondingly, the RFD could be represented as

$$\begin{aligned} Y_{\text{RFD}} &= \overline{y_1} + D(T_L - \Delta T) \\ &= \frac{D}{2}\left[T_L - T_I - \Delta T + \frac{4T_L}{P+I}\right] \\ &= \left[1 + \frac{T_L - T_I - \Delta T}{4T_L}(P+I)\right]\overline{y_e}, \end{aligned} \tag{6}$$

where ΔT is the time before the Ramsey interaction in one fountain cycle. Thus, the Y_{RFD} is directly associated with the running parameters T_I and T_L of the AFC, y_e, and PI feedback parameters ($P = 0.75$ and $I = 0.25$ in our AFC).

The recorded data of y_e for every locking period during MJD 57080-57103 are presented in Fig. 3(a). Utilizing the data in Fig. 3(a) and the statistics method from Ref. [17], we obtain the bias and uncertainty of the RFD, with the average time scale of one day, as shown in Fig. 3(b). The RFD is calculated with the bias data of Fig. 3(b), and it turns out to be $-3(2)\times10^{-16}$. Considering the type-B uncertainties evaluated in the main AFCs are of the order of 10^{-16} or even less[3,18,19], the affection of the RFD is large enough to be taken into account in the accuracy evaluation of the AFC. On the other hand, the RFD can be derived from the drift rate of the LO, according to Eq. (6), and the calculation result is -3.9×10^{-16}, which agrees with the evaluation bias (-3×10^{-16}) result within the type-B uncertainty (2×10^{-16}). It verifies the validity of the evaluation of the RFD above.

The Allan deviation of the error signal in the phase locked loop (PLL) approximately follows the line of τ^{-1}[20]. The LOL scheme is the same as the PLL and, as shown in black square of Fig. 3(c), is the Allan deviation of the RFD during MJD 57080-57103, with the fitting line of $8.8\times10^{-13}\tau^{-0.9}$ for data at the average time of less than 10^3 s. In a time scale larger than 10^5 s, the curve of Allan deviation tends to become flat around 1×10^{-16}, which is ascribed to the time variation of the frequency drift rate of the LO. The effect that the frequency drift changes with time will affect the bias of the RFD, and in turn induce a confusion in accuracy evaluation. To reduce the effect caused by the time-variation of the RFD, a sectionalized post-process method is adopted. In this method, we divide the RFD data into sections with the same time scale of a day ($\sim10^5$ s). The frequency bias was literally subtracted from the RFD for every time section. The Allan deviation of the RFD after the sectionalized post-process is then shown in the red diamond of Fig. 3(c). It is inferred that two Allan deviation curves coincide well with each other at the average time less than 10^5 s. However, the Allan deviation can be obviously reduced at an average time larger than 2×10^5 s with respect to the original data, and ultimately reduced by about one order of magnitude at an average time of 4×10^5 s. Thus, in a larger time scale, the sectionalized post-process method is more effective in calibrating the RFD, and the total evaluation accuracy and precision of the atomic fountain is believed to be improved.

Additionally, since the frequency error is monitored in real time, the RFD could be compensated by adding a

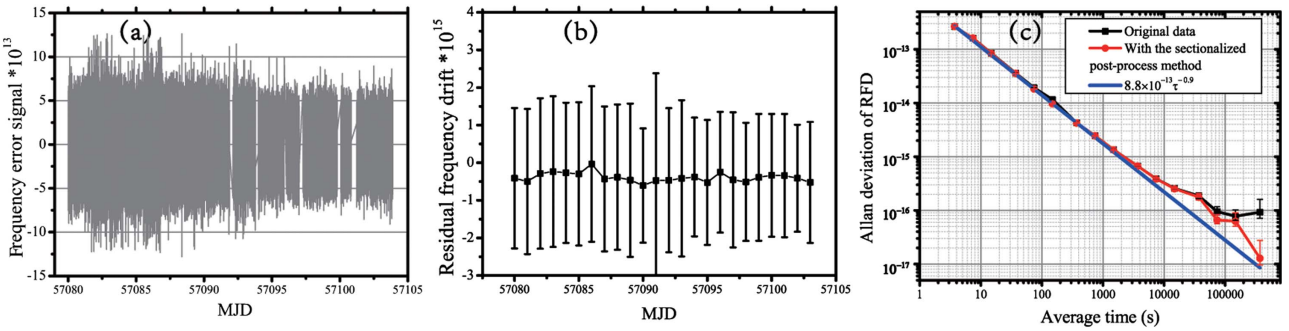

Fig. 3. (a) Recorded fractional frequency error signal y_e; (b) evaluation result of the bias and uncertainty of RFD: $-3(2) \times 10^{-16}$, with the average time of a day; (c) the Allan deviation of the RFD. Red square: with the sectionalized post-process method; black diamond: original data without the sectionalized post-process method. In the sectionalized method, the data are divided into the same time scale of a day. All data in Fig. 3 are generated in LOL during MJD 57080-57103.

RFD-dependent voltage feedback synchronously. We have adopted such a compensation scheme and gained a better Allan deviation of the RFD, and the corresponding result will be represented in another paper.

In conclusion, we directly lock the LO on the resonance spectrum of our rubidium atomic fountain. The short-term fractional frequency stability of the locked LO compared with an active H-maser is $2.7 \times 10^{-13}\tau^{-1/2}$, which reaches 1.8×10^{-15} at the average time of 40000 s. We set up a theoretical model to analyze the RFD and evaluate that the RFD is $-3(2) \times 10^{-16}$ during MJD 57080-57103. We also propose a sectionalized post-process method of calibrating the RFD, which leads to an order of magnitude reduction in the Allan deviation of RFD. This sectionalized post-process method may apply to the calibration of frequency drift of the ultra stable laser locked by the ultra stable Fabry–Perot cavity in the optical clocks[21].

This work was supported by the National Natural Science Foundation of China under Grant Nos. 61275204, 91336105, and 11404353.

References

1. R. Wynands and S. Weyers, Metrologia **42**, S64 (2005).
2. T. P. Heavner, S. R. Jefferts, E. A. Donley, J. H. Shirley, and T. E. Parker, Metrologia **42**, 411 (2005).
3. J. Guéna, M. Abgrall, D. Rovera, P. Laurent, B. Chupin, M. Lours, G. Santarelli, P. Rosenbusch, M. E. Tobar, R. Li, K. Gibble, A. Clairon, and S. Bize, IEEE Trans. Ultrason. Ferroelectr. Freq. Control **59**, C3 (2012).
4. S. Peil, J. L. Hanssen, T. B. Swanson, J. Taylor, and C. R. Ekstrom, Metrologia **51**, 263 (2014).
5. BIPM, BIPM Annual Report on Time Activities (2013).
6. J. Guéna, M. Abgrall, A. Clairon, and S. Bize, Metrologia **51**, 1 (2014).
7. F. Levi, D. Calonico, C. E. Calosso, A. Godone, S. Micalizio, and G. A. Costanzo, Metrologia **51**, 270 (2014).
8. K. Szymaniec, S. E. Park, G. Marra, and W. Chałupczak, Metrologia **47**, 363 (2010).
9. S. Weyers, U. Hübner, R. Schröder, C. Tamm, and A. Bauch, Metrologia **38**, 343 (2001).
10. G. D. Rovera, M. Abgrall, and P. Laurent, in *2011 Joint Conference of the IEEE International Frequency Control and the European Frequency and Time Forum (FCS)* (2011).
11. M. Niering, R. Holzwarth, J. Reichert, P. Pokasov, Th. Udem, M. Weitz, and T. W. Hänsch, Phys. Rev. Lett. **84**, 24 (2000).
12. T. P. Heavner, E. A. Donley, F. Levi, G. Costanzo, T. E. Parker, J. H. Shirley, N. Ashby, S. Barlow, and S. R. Jefferts, Metrologia **51**, 174 (2014).
13. Oscilloquartz S.A./Rue des BrØvards 16/CH-2002 Neuchâtel, "OCXO 8607 10 times better than any other OCXO," (2010).
14. C. Shi, R. Wei, Z. Zhou, T. Li, L. Li, and Y. Wang, in *2011 Joint Conference of the IEEE International Frequency Control and the European Frequency and Time Forum (FCS)* (2011).
15. G. Santarelli, C. Audoin, A. Makdissi, P. Laurent, G. J. Dick, and A. Clairon, IEEE Trans. Ultrason. Ferroelectr. Freq. Control **45**, 887 (1998).
16. J. A. Barnes, Proc. IEEE **54**, 2 (1966).
17. P. R. Bevington and D. K. Robinson, *Data Reduction and Error Analysis for the Physical Sciences* (McGraw–Hill, 2003).
18. K. Szymaniec, S. Lea, and K. Liu, IEEE Trans.Ultrason. Ferroelectr. Freq. Control **61**, 203 (2014).
19. S. R. Jefferts, T. P. Heavner, T. E. Parker, J. H. Shirley, E. A. Donley, and N. Ashby, Phys. Rev. Lett. **112**, 050801 (2014).
20. D. Banerjee, *PLL performance, Simulation and Design* (Dog Ear Publishing, 2006).
21. P. Jia and D. Wang, Chin. Opt. Lett. **11**, 040601 (2013).